

# Bending Moduli of Charged Membranes Immersed in Polyelectrolyte Solutions

Adi Shafir\* and David Andelman<sup>†</sup>

School of Physics and Astronomy

Raymond and Beverly Sackler Faculty of Exact Sciences

Tel Aviv University, Ramat Aviv, Tel Aviv 69978, Israel

Received 5st September 2006,

DOI: 10.1039/

We study the contribution of polyelectrolytes in solution to the bending moduli of a charged membrane. Using the Helfrich free energy, within the mean field approximation, we find a non-monotonic dependence of the bending moduli on the short-range interactions between the membrane and the polyelectrolyte chains. For short-range repulsion, the membrane rigidifies. For weak short-range attraction, the membrane rigidity decreases, whereas for strong short-range attraction, the membrane rigidity increases again. The effect of added salt on the bending rigidity and membrane stability is also investigated.

## 1 Introduction

The study of interactions between charged and flexible surfaces or membranes and polyelectrolytes (PEs) in solution has generated a lot of interest in recent years. This interest is partly motivated by the importance of such interactions in biology. DNA, RNA and various proteins are charged biological macromolecules (polyelectrolytes). Understanding the interaction between these macromolecules and biological cell membranes (modeled as charged and flexible interfaces) sheds light on many important cellular processes.

Besides its biological significance, the adsorption of PEs onto charged membranes raises interesting questions about the interplay between short-range and electrostatic (long range) interactions in these multi-component charged systems. Recent works include numerical calculations [1, 2, 3, 4, 5, 6], analytical calculations [7, 8, 9, 10, 11] and scaling arguments [1, 4, 5, 12, 13].

In a previous work [14], three main regimes have been found for polyelectrolyte adsorption. (i) When the short-range interaction between the membrane and the PE chains is repulsive, the surface charge is low and the ionic strength of solution high, the polymers deplete from the charged membrane. (ii) For higher surface charges, or lower ionic strength, the polyelectrolytes adsorb on the charged membrane and screen its charges. (iii) When the short-range interactions between the membrane and the PE chains are attractive, the PE chains adsorb on the membrane, and the adsorbed layer carries a higher charge than that of the initial membrane.

The flexibility of fluid surfaces and membranes has been studied in various cases, depending on the lipid composition, tail length and molecular tilt. The contribution of the lipid charges has been investigated for membranes immersed in an ionic solution (no macromolecules) [15, 16, 17, 18, 19, 20, 21, 22, 23, 24, 25, 26]. The electrostatic contribution was found to increase the membrane rigidity, and the addi-

\*E-mail:shafira@post.tau.ac.il

<sup>†</sup>E-mail:andelman@post.tau.ac.il

tion of salt to decrease it. In a different set of studies, the adsorption of neutral polymers has been investigated by mean-field calculations [27, 29, 28, 30, 31, 32] and complemented experiments [33, 34, 35, 36]. It was found that the addition of polymers reduces the membrane rigidity.

In the present work, we study the combined system of charged chains interacting with oppositely charged and flexible membranes. Our study is similar in spirit to that done for DNA-lipid systems [37, 38], where the DNA was modeled as rigid and charged rod. The main difference is that our charged macromolecules are taken as flexible ones. The above mentioned three regimes have different effect on the rigidity and stability of the membrane. For short-range repulsive membranes, the membrane becomes rigid due to electrostatics, and its rigidity decreases with the increase of the polyelectrolyte charge. For weak short-range interactions, the membrane becomes flexible, and for strong short-range repulsion, the membrane becomes rigid again. The effect of addition of salt is also investigated.

## 2 Mean Field Equations

### 2.1 Free-Energy Formulation

Consider a bulk aqueous solution containing polyelectrolyte (PE) chains, along with their counter ions and added salt. A curved and charged membrane is placed at the origin  $|\mathbf{r}| = 0$ . In order to extract the membrane elastic moduli, we take the membrane shape to be either spherical or cylindrical with radius  $R$ . The free energy for the combined system has been formulated before [1], and can be written as a sum of four contributions  $F_{\text{tot}} = F_{\text{pol}} + F_{\text{ions}} + F_{\text{el}} + F_{\text{int}}$ .

The polymer free energy,  $F_{\text{pol}}$ , is:

$$F_{\text{pol}} = \int_V d\mathbf{r} \left[ \frac{a^2 \phi_b^2}{6} |\nabla \eta|^2 + \Sigma - \Sigma_b \right], \quad (1)$$

where  $a$  is the monomer size,  $\phi_b^2$  is the monomer bulk concentration,  $\phi^2 \equiv \phi_b^2 \eta^2(x)$  is the local monomer concentration. The free energy

is given in terms of  $k_B T$ , and the integration is carried out over the entire volume outside the sphere/cylinder,  $|\mathbf{r}| > R$ . The first term in Eq. (1) accounts for the chain elasticity. The second and third terms account for the excluded volume interactions in the solution and in the bulk, respectively:

$$\begin{aligned} \Sigma a^3 &= (1 - a^3 \phi_b^2 \eta^2) \log(1 - a^3 \phi_b^2 \eta^2) - \\ &\quad \frac{1}{2} (v - a^3) (1 - a^3 \phi_b^2 \eta^2) \phi_b^2 \eta^2 + \\ &\quad a^3 \phi_b^2 \left[ \log(1 - a^3 \phi_b^2) + \right. \\ &\quad \left. \frac{1}{2} (v a^{-3} + 1) - (v - a^3) \phi_b^2 \right] \eta^2 \quad (2) \\ \Sigma_b a^3 &= (1 - a^3 \phi_b^2) \log(1 - a^3 \phi_b^2) - \\ &\quad \frac{1}{2} (v - a^3) (1 - a^3 \phi_b^2) \phi_b^2 + \\ &\quad a^3 \phi_b^2 \left[ \log(1 - a^3 \phi_b^2) + \right. \\ &\quad \left. \frac{1}{2} (v a^{-3} + 1) - (v - a^3) \phi_b^2 \right] \quad (3) \end{aligned}$$

where  $v$  is the excluded volume coefficient. For  $\phi_b^2 \eta^2 \ll a^{-3}$  the above expression can be expanded to the well known  $\frac{1}{2} v \phi_b^4 (\eta^2 - 1)^2$ , which is commonly used for the excluded volume interaction.

The small ion contribution to the entropy is:

$$F_{\text{ions}} = \sum_{i=\pm} \int_V d\mathbf{r} \left[ c_i \log \frac{c_i(x)}{c_b^i} - c_i(x) + c_b^i \right] \quad (4)$$

where  $c_{\pm}$  and  $c_b^{\pm}$  are the local and bulk concentrations of the  $\pm$  small ions, respectively. The third contribution to free energy, the electrostatic free-energy, is:

$$\begin{aligned} F_{\text{el}} &= \int_V d\mathbf{r} (c_+ - c_- + f \phi_b^2 \eta^2) \zeta - \\ &\quad \frac{1}{8\pi l_B} \int_V d\mathbf{r} |\nabla \zeta|^2 + \int_{|\mathbf{r}|=R} d\mathbf{A} \sigma \zeta \quad (5) \end{aligned}$$

where  $\zeta \equiv e\psi/k_B T$  is the renormalized electrostatic potential,  $f$  is the fraction of charged monomers and  $l_B \equiv e^2/\epsilon k_B T$  is the Bjerrum length. The first integral accounts for the interactions between the positive ions, negative small ions and the monomer charges with the

electrostatic potential. The second integral accounts for the self-energy of the electrostatic field and the third to the interaction between the surface charge and the electrostatic potential. Note that the third integral is taken only over the charged body surface,  $|\mathbf{r}| = 0$ .

The last part of the free energy is the short-range interaction of the PE chains with the membrane:

$$F_{\text{int}} = -\frac{a^2}{6d} \int_{|\mathbf{r}|=R} d\mathbf{A} \phi_b^2 \eta_s^2 \quad (6)$$

where  $\eta_s \equiv \eta(|\mathbf{r}| = R)$  is the renormalized monomer concentration on the surface. This term stands for a general short-range interaction, where the interaction strength is determined by the phenomenological constant  $d^{-1}$ , which has dimensions of inverse length.

Minimization of the total free energy  $F_{\text{tot}} = F_{\text{pol}} + F_{\text{ions}} + F_{\text{el}} + F_{\text{int}}$  yields the following mean-field equations:

$$\nabla^2 \zeta = \lambda_D^{-2} \sinh \zeta + k_m^2 (e^\zeta - \eta^2) - 4\pi l_B \sigma \delta(|\mathbf{r}| - R) \quad (7)$$

$$\frac{a^2}{6} \nabla^2 \eta = \Lambda(\eta) \eta - f \zeta \eta - \frac{a^2}{6d} \delta(|\mathbf{r}| - R) \eta \quad (8)$$

where  $\lambda_D = (8\pi l_B c_{\text{salt}})^{-1/2}$  is the Debye-Hückel length scale for the screening of the electrostatic potential in the presence of added salt and  $k_m^{-1} = (4\pi l_B \phi_b^2 f)^{-1/2}$  is the corresponding length for the potential decay due to counterions. Note that the actual decay of the electrostatic potential is determined by a combination of salt, counterions, and polymer screening effects. The excluded volume interaction is taken into account using the function:

$$\Lambda(\eta) = \log(1 - \phi_b^2 a^3) - \log(1 - \phi_b^2 a^3 \eta^2) + (v - a^3) \phi_b^2 (\eta^2 - 1) \quad (9)$$

which represents the full excluded volume interaction.

The solution of Eqs. (7) and (8) requires four boundary conditions. Two of the boundary

conditions are taken far from the membrane, where the monomer concentration and electrostatic potential retrieve their bulk values  $\eta(|\mathbf{r}| \rightarrow \infty) \rightarrow 1$  and  $\zeta(|\mathbf{r}| \rightarrow \infty) \rightarrow 0$ . The other two boundary conditions account for the interaction with the charged membrane, and can be obtained by integrating Eqs (7,8) from  $|\mathbf{r}| = R$  to a small distance from the membrane, yielding:

$$\hat{\mathbf{n}} \cdot \nabla \zeta|_{|\mathbf{r}|=R} = -4\pi l_B \sigma \quad (10)$$

$$\hat{\mathbf{n}} \cdot \nabla \eta|_{|\mathbf{r}|=R} = -d^{-1} \eta_s \quad (11)$$

Equation (10) is the usual electrostatic boundary condition for a given surface charge density, while Eq. (11) is the Cahn - de Gennes boundary condition [39], which is often used for calculating polymer profiles [28, 29, 27].

For large  $R$ , the total free-energy can be expanded around its flat surface value in the following way [41]:

$$F_{\text{tot}} = \int_{|\mathbf{r}|=R} d\mathbf{A} \left[ f_0 + \frac{1}{2} \delta\kappa \left( c_1 + c_2 - \frac{2}{R_0} \right)^2 + \delta\kappa_G c_1 c_2 \right] \quad (12)$$

where  $F_{\text{tot}}$  is the total free energy (in units of  $k_B T$ ),  $f_0$  is the free energy per unit area of a solution in contact with a planar surface that has the same system parameters, and  $c_1, c_2$  are the radii of curvature for the membrane. For spherical surfaces the radii of curvature are  $c_1 = c_2 = 1/R$ , while for a cylindrical surface  $c_1 = 1/R, c_2 = 0$ . The parameters  $\delta\kappa$  and  $\delta\kappa_G$  are the contributions of the PE (and salt) solution to the mean and Gaussian curvature moduli of the membrane, respectively, in units of  $k_B T$ . Namely,  $\kappa = \kappa^0 + \delta\kappa$  and  $\kappa_G = \kappa_G^0 + \delta\kappa_G$  include the intrinsic values as well as the contributions coming from the solution. Throughout this paper we will consider only the changes in the elastic moduli  $\kappa, \kappa_G$  with respect to their bare values. An increase in the mean curvature modulus  $\delta\kappa$  increases the membrane rigidity, while an increase in the Gaussian modulus  $\delta\kappa_G$  makes saddle points on the membrane more favorable.

The parameter  $R_0$  is the radius of spontaneous curvature for the membrane, which is dependent on the exact chemical composition of the membrane. For a positive  $R_0$ , the membrane bends towards the solution, while for negative  $R_0$  it bends away from solution. In the usual case where the same solution is in contact with both sides of the membrane, the spontaneous curvature vanishes due to symmetry. In this paper, we do not calculate the spontaneous curvature but rather focus on the bending moduli  $\delta\kappa$  and  $\delta\kappa_G$ .

## 2.2 Numerical Procedure

Eqs. (7)-(11) are solved numerically for the cases of a charged sphere and a charged cylinder. The numerical procedure followed the relaxation scheme [40], as was described in previous publications [4, 5]. For each solution, we calculated the total free energy per unit area for the cases of a spherical membrane  $f_S$  and a cylindrical membrane  $f_C$ . The contributions of the polyelectrolyte solution to the mean and Gaussian curvatures are then calculated by expanding  $f_C$ ,  $f_S$  to second order in  $1/R$ :

$$f_S = f_0 + \frac{A_S}{R} + \frac{B_S}{R^2} \quad (13)$$

$$f_C = f_0 + \frac{A_C}{R} + \frac{B_C}{R^2} \quad (14)$$

The contributions of the solution to the curvature moduli are given by:

$$\delta\kappa = 2B_C \quad (15)$$

$$\delta\kappa_G = B_S - 4B_C. \quad (16)$$

A surface is stable under long wave bending fluctuations only when  $\kappa > 0$ , and against spontaneous vesiculation (topological change) when  $2\kappa + \kappa_G > 0$  [23]. In the following we show that the contribution of the PE solution to the stability of a charged surface depends on the amount of added salt, and has a non-monotonic dependence on the short-range interactions between the membrane and the polyelectrolyte.

## 3 Numerical Results

We find five different regimes for the surface bending moduli. Two regimes occur for strong short-range repulsion, and three for short-range attraction. These five regimes are presented below.

### 3.1 Short Range Repulsive Membranes

For strongly repulsive surfaces, the adsorption of PE chains to the membrane is aimed mostly to screen its surface charges. The charges on the membrane increase the membrane rigidity, due to the long-range repulsion between them, increasing the mean curvature modulus  $\kappa$ . The screening of these charges, in turn, causes this modulus to decrease. There are two regimes for the case of short range repulsive membranes: (i) the low salt regime, where the surface charges are balanced by the adsorbed monomer charges, and (ii) the high salt regime, where the salt ions screen the surface charges and the monomers deplete.

In a previous publication [4] we showed that the screening length of the electrostatic potential depends strongly on the amount of added salt. We also showed that for small amounts of added salt the surface charges are screened mainly by the adsorbed monomer charges. In this case the free-energy per unit area of such a solution near a flat surface scales like  $f_A \sim |\sigma|^{5/3} f^{-1/3} a^{2/3} l_B^{2/3}$  and the screening length scales like  $D \sim a^{2/3} / (fl_B |\sigma|)^{1/3}$  [4]. For high amounts of added salt, the screening is done mostly by small ions and the PE chains deplete. In this case, the free energy is similar to that of an ionic solution [23], namely the screening length is  $\lambda_D$  and the free energy per unit area for the case of a flat surface is  $f_D \sim |\sigma|^2 l_B \lambda_D$ . The transition from depletion to adsorption regimes occurs when the screening length due to monomer adsorption becomes smaller than the one for small ion adsorption, i.e., when  $\lambda_D > D$ .

The adsorption-depletion crossover creates two regimes for the short-range repulsive membranes. In the low salt regime, monomers are adsorbed to the membrane, and the length scale

for the adsorption is  $D$ . In this case, we expect the free energy of the curved membrane (per unit area) to scale like  $f_{\text{tot}} = f_A h(D/R)$ . Expanding  $f$  to second order in  $R^{-1}$  and comparing to Eq. (12) shows that both curvature moduli scale like:

$$\delta\kappa, \delta\kappa_G \sim f_A D^2 \sim \frac{|\sigma| a^2}{f} \quad (17)$$

For higher salt concentrations, the membrane interacts only with the small ions, and the polymer chains are driven away toward the bulk. The curvature moduli are the same as in a simple ionic solution [15, 16, 17, 19, 23], where:

$$\delta\kappa, \delta\kappa_G \sim f_D \lambda_D^2 \sim |\sigma|^2 l_B \lambda_D^3. \quad (18)$$

Both regimes are seen in our numerical results. In Fig. 1 we present the values of  $\delta\kappa$  and  $\delta\kappa_G$  as a function of the amount of added salt, in the case of strongly repulsive membranes  $d^{-1} = -5 \text{ \AA}^{-1}$ . As can be seen, the values of  $\delta\kappa$  and  $\delta\kappa_G$  are very low, and decrease with the amount of added salt. Two regimes can be distinguished: a low salt adsorption regime and a high salt depletion regime. The surface charge dependence of  $\delta\kappa, \delta\kappa_G$  are presented in Fig. 2. For the low salt regime, the values of the curvature moduli scale like  $\delta\kappa \sim |\sigma|$  while for the high salt regime  $\delta\kappa \sim |\sigma|^2$ , in agreement with the above model. For both regimes, the contribution to the Gaussian bending modulus  $\delta\kappa_G$  is negative, resulting from the electrostatic repulsion between the membrane constituents [18]. As can be seen, this negative contribution also decreases with the screening of the electrostatic interactions. For all salt concentrations, the contribution of the PE solution to the curvature moduli is very small in comparison to the intrinsic curvature moduli of fluctuating membranes, which is of the order of  $20k_B T$  ( $10k_B T$  per leaflet). The contribution of the PE solution to the vesiculation stability  $2\delta\kappa + \delta\kappa_G$  is always positive, even for very low salt concentrations, in contrast to the pure ionic solution results [20, 21, 22]. The low salt regime of the ionic solutions, in which the contribution to  $2\delta\kappa + \delta\kappa_G$  is negative, is replaced here by the adsorption regime, in which this contribution is still positive.

## 3.2 Short Range Attractive Membranes

When the PE chains have short-range attraction to the membrane, the surface charge screening stops being the sole reason for the adsorption. In previous publications [5, 6], the adsorbed amount of PEs has been studied in detail for short-range attractive surfaces. Its charge was shown to exceed the bare surface charge significantly for strong short-range interactions, and to exceed it mildly for weak short-range interactions. The combined charge of the membrane and the adsorbed PEs is, therefore, opposite to the initial surface charge, and its magnitude may be much higher than the initial membrane charge.

In Fig. 3 we show the numerical dependence of  $\delta\kappa, \delta\kappa_G$  on the short-range interaction parameter  $d^{-1}$ , for several salt concentrations. For repulsive membranes  $d^{-1} < 0$ , Fig. 3 shows the same behavior as in Fig. 1, namely  $\delta\kappa > 0, \delta\kappa_G < 0$ . For  $d^{-1} \geq 0$ , however, we find two regimes for the curvature moduli  $\delta\kappa, \delta\kappa_G$ : (i) a high salt (weak attraction) regime, and (ii) a low salt (strong attraction) regime. In the first regime, the membrane mean curvature modulus decreases  $\delta\kappa < 0$  and its Gaussian curvature modulus increases  $\delta\kappa_G > 0$ . In the second, the opposite occurs, the membrane becomes rigid  $\delta\kappa > 0$  and the Gaussian modulus decreases.

It is important to note that we do not have good scaling or analytical approximations for the short-range attractive regimes. Our explanations for the numerical results are more qualitative than in the short-range repulsion regimes. However, we can understand the physics behind these results through analogies with other systems. These analogies are described below.

### 3.2.1 High Salt - Weak Attraction Regime

In this regime, the amount of salt added to the solution is very high, and the charges of both the PE chains and the membrane are screened over very short length scales. The PE solution behaves qualitatively like a neutral polymer solution. The width of the adsorbed layer depends

on the shorter length scale between the two adsorption length scales: (i)  $d$ , the length scale for short-range attraction from Eq. (11), and (ii)  $\xi \equiv a/\sqrt{v\phi_b^2}$ , the Edwards correlation length for neutral polymer adsorption. In our model, we use an almost theta solvent  $0 < v\phi_b^2 \ll 1$ , so we assume that the shorter length scale is always  $d$ .

For low  $d^{-1}$  and high amounts of added salt, we find a decrease in the mean curvature modulus due to the polymer adsorption  $\delta\kappa < 0$ , as well as in  $2\delta\kappa + \delta\kappa_G$ . This surprising result can be explained by analogy to the neutral polymer case. In other publications [27, 28, 29], it was shown that neutral polymer solutions decrease the membrane rigidity as well as  $2\delta\kappa + \delta\kappa_G$ . The same results are found in this regime. Similarly to the neutral polymer case, we also find here a positive contribution to the Gaussian bending modulus.

The analogy to neutral polymers arises since the high amount of added salt screens both the surface and the PE charges, so their effective interaction becomes short-range, and they behave almost as neutral polymers. The increase in  $\delta\kappa_G$ , in this case, derives from the effective attraction between membrane constituents, which results from their short-range attraction to the PE chains. The analogy to neutral polymers requires the screening length scale for the electrostatic interactions to be much smaller than the layer width  $\lambda_D < d$ , which requires high amounts of added salt and low short-range attraction. For stronger short-range interactions, the layer width decreases, and the long-range (electrostatic) interactions between monomers becomes important. In this case, the analogy to neutral polymers brakes down, and  $\delta\kappa$ ,  $2\delta\kappa + \delta\kappa_G$  start to increase back. For higher  $d^{-1}$ , both  $\delta\kappa$ ,  $2\delta\kappa + \delta\kappa_G$  become positive again, marking the crossover to the strong attraction regime.

It is important to note that we do not see the same  $d^{-1}$  dependence in the numerical results as in the neutral polymer case, since in our case the interaction between the monomers is not the simple excluded volume one. However, this analogy can shed some light on the origin of the decrease in  $\delta\kappa$ ,  $2\delta\kappa + \delta\kappa_G$ . The crossover between the weak and strong attraction regimes

indeed follows the above prediction, as seen in Fig. 3.

### 3.2.2 Low Salt - Strong Attraction Regime

As the short-range interactions increase, the adsorbed layer width decreases. When the adsorbed layer width is smaller than the electrostatic screening length, the system can be viewed as a renormalized charged surface, containing both the bare surface charges and the adsorbed PE charges, in a weak ionic solution. The renormalized surface interacts with the ionic solution in the same manner as the bare membrane. The contribution to the mean curvature modulus increases again, due to the electrostatic repulsion between the adsorbed monomers.

There are two regimes for the contribution to the vesiculation stability  $2\delta\kappa + \delta\kappa_G$  in ionic solutions [23], depending on the surface charge. For weakly charged surfaces  $c_{\text{salt}} \gg l_B |\sigma|^2$ , the contribution to the membrane rigidity and to  $2\delta\kappa + \delta\kappa_G$  is positive [17, 19], while for highly charged surfaces  $c_{\text{salt}} \ll l_B |\sigma|^2$  the contribution to  $\delta\kappa$  is positive and to  $2\delta\kappa + \delta\kappa_G$  is negative [20, 21]. In our membranes, for low enough attractive short-range interactions the renormalized surface charge is low, and  $2\delta\kappa + \delta\kappa_G > 0$ . For stronger short-range interactions, the renormalized surface charge increases and  $2\delta\kappa + \delta\kappa_G < 0$ . The magnitude of  $\delta\kappa$ ,  $\delta\kappa_G$  in this case can amount to several  $k_B T$ , which is a significant contribution to the membrane curvature moduli, as can be seen in Fig. 4.

The full dependence of  $2\delta\kappa + \delta\kappa_G$  on the short-range interactions is presented in Fig. 5. Four regimes are presented in the low salt curve. For large negative  $d^{-1}$  (repulsive short-range interactions), the contribution to  $2\delta\kappa + \delta\kappa_G$  is positive, meaning that the PE solution makes the vesiculation less favorable. For low positive  $d^{-1}$ , it changes sign  $2\delta\kappa + \delta\kappa_G < 0$ , analogous to a neutral polymer solution. As  $d^{-1}$  increases beyond  $\lambda_D^{-1}$ , the sign of  $2\delta\kappa + \delta\kappa_G$  changes again and becomes positive, analogous to a surface with a weak renormalized charge. For very high  $d^{-1}$ , the renormalized surface charge increases,

and  $2\delta\kappa + \delta\kappa_G$  becomes negative again.

We show only three of the regimes in the high salt case, the repulsive surface regime, the low  $d^{-1}$  regime where  $2\delta\kappa + \delta\kappa_G < 0$  and the intermediate  $d^{-1}$  regime, where the contribution to  $2\delta\kappa + \delta\kappa_G$  is positive. It is important to see that for high amounts of added salt, the increase in  $\delta\kappa$  with  $d^{-1}$  indeed begins when  $\lambda_D^{-1} \simeq d^{-1}$ , marking the crossover from the second and the third regimes as is expected from the above analysis. Since in this regime the adsorbed amount of monomers increases strongly with salt [5], the numerical calculation for high  $d^{-1}$  becomes extremely difficult, and we could not retrieve the fourth, high  $d^{-1}$  regime ( $\delta\kappa > 0$ ,  $2\delta\kappa + \delta\kappa_G < 0$ ) numerically. Since such high short-range interactions are necessary for this regime, we do not think that the existence of this regime for very high salt concentrations can be verified experimentally.

A phase diagram summarizing our results for the different regimes is presented in Fig. 6. For strongly repulsive membranes, both  $\delta\kappa$  and  $2\delta\kappa + \delta\kappa_G$  are positive. For low salt concentrations, the curvature moduli depend on the polymer adsorption, and are weakly affected by the amount of salt (regime S1). For high salt concentrations, the curvature moduli depend strongly on the salt concentration and less on the polymer charge (S2). As the short-range interaction becomes more attractive, the membranes become less rigid  $\delta\kappa < 0$  and the vesiculation becomes more favorable  $2\delta\kappa + \delta\kappa_G < 0$  (U1). When the short range attraction becomes even stronger, the rigidity of the membrane increases back, and  $2\delta\kappa + \delta\kappa_G > 0$  again (S3). Finally for very strong short-range attraction and low amounts of added salt, the bending rigidity increases but  $2\delta\kappa + \delta\kappa_G < 0$  (U2).

## 4 Conclusions

In this paper we find that the interaction between charged polymers (PE) and oppositely charged and flexible membrane depends both on electrostatic and short-range interactions. A non-monotonic dependence of the curvature moduli is obtained as function of the short-

range interaction between the membrane and the PE chains. We show that for repulsive as well as *weak* attractive interactions, the contribution of the PE solution to the membrane curvature moduli is small (in units of  $k_B T$ ). For strong short-range attraction, however, a significant contribution to the curvature moduli is obtained and can reach several  $k_B T$ . It is important to note that we find five regimes characterizing the behavior of the bending moduli, rather than the three regimes previously found for the corresponding flat surface [14].

All our results are derived using mean-field theory, which neglects the effects of correlations and fluctuations in the polymer and small ion concentrations. We also use the ground state dominance approximation, which is accurate for very long chains. It will be of value to extend the results obtained here for true bilayer membranes composed of two leaflets. This will require modeling the finite thickness of the bilayer by a different dielectric constant. Another extension is to consider the effect of the PE solution on  $R_0$  — the spontaneous radius of curvature.

A recent paper [43] showed that the bending rigidity of lipid membranes also decreases due to DNA adsorption. Future experimental works may shed further light on different elastic regimes — especially in the cases where the contribution to the elastic moduli is substantial — and verify their validity.

*Acknowledgments:* The authors wish to thank Michael Kozlov for helpful discussions. Support from the Israel Science Foundation (ISF) under grant no. 160/05 and the US-Israel Binational Foundation (BSF) under grant no. 287/02 is gratefully acknowledged.

**Adi Shafir,<sup>a</sup> David Andelman<sup>a</sup>**  
<sup>a</sup> *School of Physics and Astronomy*

*Raymond and Beverly Sackler Faculty of Exact  
Sciences  
Tel Aviv University, Ramat Aviv, Tel Aviv  
69978, Israel.*

## References

- [1] I. Borukhov, D. Andelman, H. Orland, *Macromolecules*, 1998, **31**, 1665; *Europhys. Lett.*, 1995, **32**, 499.
- [2] I. Borukhov, D. Andelman, H. Orland, *Eur. Phys. J. B*, 1998, **5**, 869.
- [3] I. Borukhov, D. Andelman, H. Orland, *J. Phys. Chem. B*, 1999, **103**, 5042.
- [4] A. Shafir, D. Andelman, R.R. Netz, *J. Chem. Phys.*, 2003, **119**, 2355.
- [5] A. Shafir, D. Andelman, *Phys. Rev. E*, 2004, **70**, 061804.
- [6] Q. Wang, *Macromolecules*, 2005, **38**, 8911.
- [7] F.W. Wiegels, *J. Phys A: Math. Gen.*, 1977, **10**, 299.
- [8] M. Muthukumar, *J. Chem. Phys.*, 1987, **86**, 7230.
- [9] J.F. Joanny, *Eur. Phys. J. B.*, 1999, **9**, 117.
- [10] R. Varoqui, *J. Phys. II (France)*, 1993, **3**, 1097.
- [11] R. Varoqui, A. Johner, A. Elaissari, *J. Chem. Phys.*, 1991, **94**, 6873.
- [12] O.V. Borisov, E.B. Zhulina, T.M. Birshtein, *J. Phys. II (France)*, 1994, **4**, 913.
- [13] A.V. Dobrynin, A. Deshkovski, M. Rubinstein, *Macromolecules*, 2001, **34**, 3421.
- [14] A. Shafir, D. Andelman, *Phys. Rev. E.*, 2006) (accepted).
- [15] D. Bensimon, F. David, S. Leibler, A. Pumir, *J. Phys. (France)*, 1990, **51**, 689.
- [16] A. Fodgen, B. W. Ninham, *Langmuir*, 1991, **7**, 590.
- [17] M. Winterhalter, W. Helfrich, *J. Phys. Chem.*, 1988, **92**, 6865.
- [18] M. Winterhalter, W. Helfrich, *J. Phys. Chem.*, 1992, **96**, 327.
- [19] M. Kiometzis, H. Kleinert, *Phys. Lett. A*, 1989, **140**, 520.
- [20] H.N.W. Lekkerkerker, *Physica A*, 1989, **159**, 319.
- [21] D. J. Mitchell, B. W. Ninham, *Langmuir*, 1989, **5**, 1121.
- [22] A. Fodgen, D. J. Mitchell, B. W. Ninham, *Langmuir*, 1990, **6**, 159.
- [23] D. Andelman, in *Handbook of Biological Physics: Structure and Dynamics of Membranes*, Vol. 1B, ed. R. Lipowsky and E. Sackmann, Elsevier Science B.V., Amsterdam, 1995, Chap. 12, p. 603.
- [24] H. von Berlepsch, R. de Vries, *Eur. Phys. J. E*, 2000, **1**, 141.
- [25] P. A. Barneveld, D. E. Hesselink, F. A. M. Leermakeers, J. Lyklema, J. M. H. M. Scheutjens, *Langmuir*, 1994, **10**, 1084.
- [26] M. M. A. E. Claessens, B. F. van Oort, F. A. M. Leermakers, F. A. Hoekstra, M. A. Cohen Stuart, *Biophys. J.*, 2004, **87**, 3882.
- [27] J. Brooks, C. Marques, M. Cates, *Europhys. Lett.*, 1991, **14**, 713; *J. Phys. II (France)*, 1991, **1**, 673.
- [28] F. Clement, J-F. Joanny, *J. Phys. II (France)*, 1997, **7**, 973.
- [29] K.I. Skau, E.M. Blokhuis, *Eur. Phys. J. E*, 2002, **7**, 13.
- [30] C. Heidgarst, R. Lipowsky, *J. Phys II (France)*, 1996, **6**, 1465.
- [31] W. Sung, S. Lee, *Europhys. Lett.*, 2004, **68**, 596.
- [32] M. Breidenich, R. R. Netz, R. Lipowsky, *Eur. Phys. J. E*, 2001, **5**, 403.
- [33] G. Bouglet, C. Liguore, A.M. Bellocq, E. Dufourc, G. Mosser, *Phys. Rev. E.*, 1998, **57**, 834.
- [34] J. Appell, C. Liguore, G. Porte, *J. Stat. Mech.: Theory and Exp.*, 2004, P08002.

- [35] G. Gompper, H. Endo, M. Mihailescu, J. Allgaier, M. Monkenbusch, D. Richter, B. Jakobs, T. Sottmann, R. Strey *Europhys. Lett.*, 2001, **56**, 683.
- [36] M. Maugey, A.M. Bellocq, *Langmuir*, 2001, **17**, 6740.
- [37] S. May, D. Harries, A. Ben-Shaul, *Biophys. J.*, 2000, **78**, 1681.
- [38] D. Harries, S. May, W.M. Gelbart, A. Ben-Shaul, *Biophys J.*, 1998, **75**, 159.
- [39] P.G. de Gennes, *Macromolecules*, 1981, **14**, 1637.
- [40] W.H. Press, B.P. Flannery, S.A. Teukolsky, W.T. Vetterling, *Numerical Recipes in C: The Art of Scientific Computing*, Cambridge University, Cambridge, 1992, Chap. 17, p. 762.
- [41] W. Helfrich, *Z. Naturforsch.*, 1973, **28c**, 693.
- [42] K.I. Skau, E.M. Blokhuis, *Macromolecules*, 2003, **36**, 4637.
- [43] A. Frantescu, S. Kakorin, K. Toensing, E. Neumann, *Phys. Chem. Chem. Phys.*, 2005, **7**, 4126.

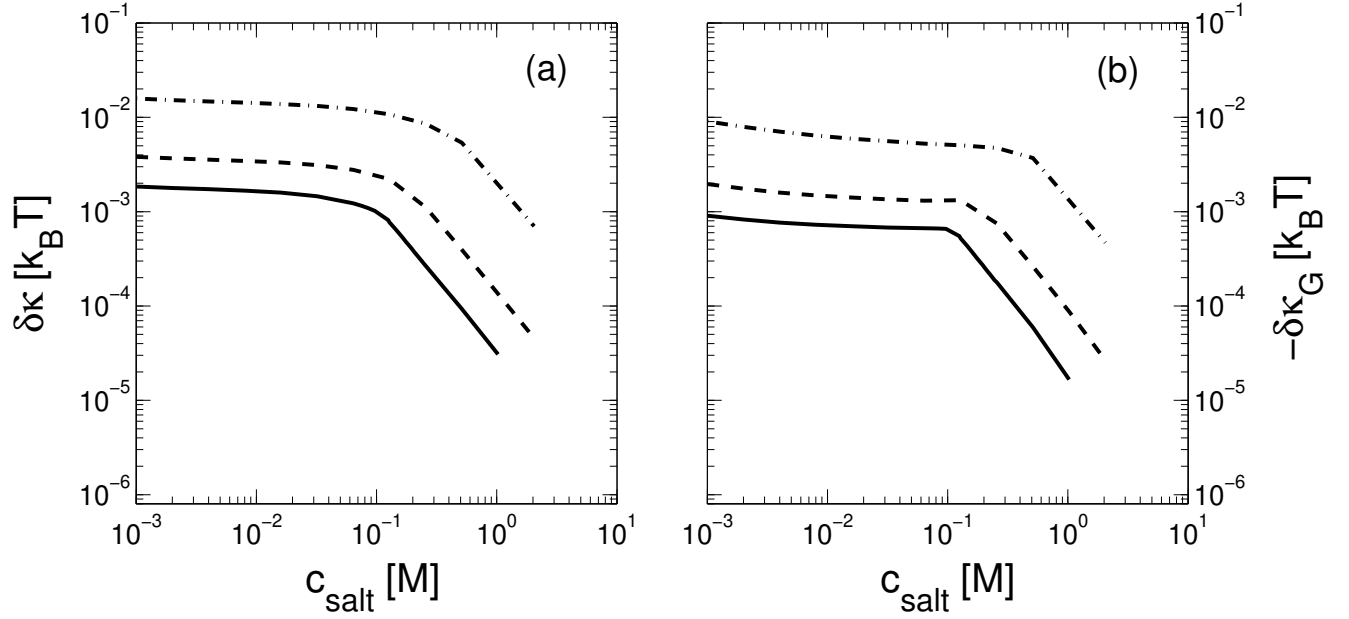


Figure 1: The mean and Gaussian curvature moduli  $\delta\kappa$  and  $\delta\kappa_G$ , respectively, are presented as functions of the amount of added salt, for the case of short-range repulsive interactions  $d^{-1} = -5$ . In both plots, the solid line corresponds to  $|\sigma| = 2 \cdot 10^{-4} \text{ \AA}^{-2}$ , the dashed line to  $|\sigma| = 4 \cdot 10^{-4} \text{ \AA}^{-2}$  and the dashed-dotted line to  $|\sigma| = 1.5 \cdot 10^{-3} \text{ \AA}^{-2}$ . Other parameters used were  $a = 5 \text{ \AA}$ ,  $f = 0.5$ ,  $v = 50 \text{ \AA}^3$ ,  $\phi_b^2 = 10^{-8} \text{ \AA}^{-3}$ ,  $T = 300 \text{ K}$  and  $\varepsilon = 80$ . As can be seen,  $\delta\kappa > 0$  and  $\delta\kappa_G < 0$  for all salt concentrations. Two regimes can be distinguished, a low salt regime where both  $\delta\kappa$  and  $\delta\kappa_G$  depend only weakly on the salt concentration, and a high salt regime where the addition of salt strongly decreases both  $\delta\kappa$  and  $\delta\kappa_G$ .

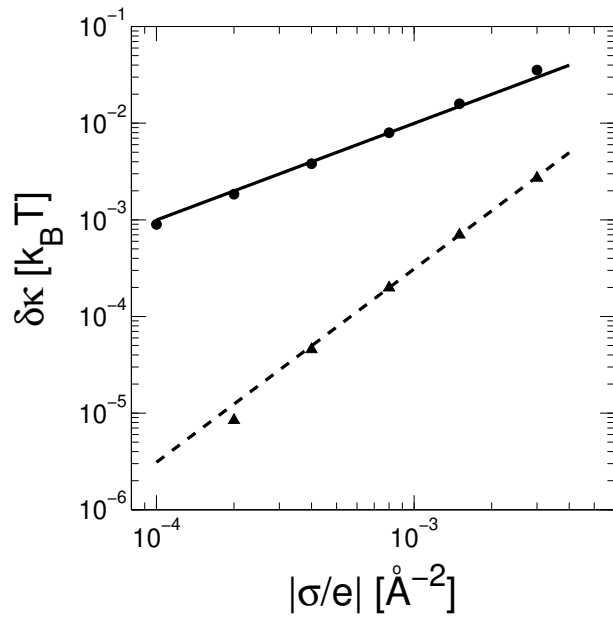


Figure 2: The dependence of  $\delta\kappa$  on the surface charge is presented for the case of repulsive membranes. The square and triangular markers are the numerically calculated  $\delta\kappa$  for  $c_{\text{salt}} = 1$  mM and  $c_{\text{salt}} = 2.0$  M respectively. Other parameters are the same as in Fig. 1. The solid and dashed lines scale as  $|\sigma|$  and  $|\sigma|^2$ , respectively. As can be seen, for low salt concentrations the curvature modulus scales like  $|\sigma|$ , and for high salt concentrations like  $|\sigma|^2$ , in agreement with Eqs. (17,18).

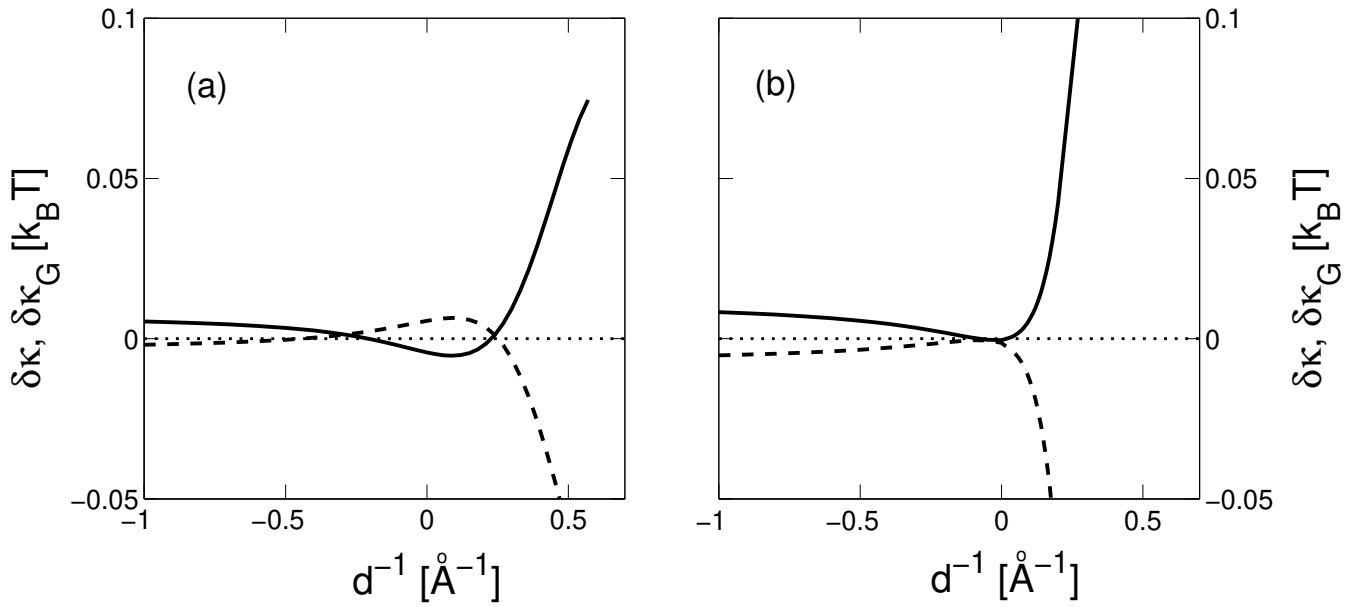


Figure 3: The  $d^{-1}$  dependence of  $\delta\kappa$  and  $\delta\kappa_G$  is presented for two salt concentrations: (a)  $c_{\text{salt}} = 0.1 \text{ M}$  and (b)  $c_{\text{salt}} = 0.1 \text{ mM}$ . All other parameters are the same as in Fig. 1. In both plots, the solid line corresponds to  $\delta\kappa$  and the dashed one to  $\delta\kappa_G$ . Both plots show three regimes for both curvature moduli. For  $d^{-1} < 0$  we see  $\delta\kappa > 0$  and  $\delta\kappa_G < 0$ , for  $d^{-1} \sim 0$  the sign of both is inverted, and for  $d^{-1} \gg 0$  both signs return to the original. The magnitude of both moduli is very small for this parameter range.

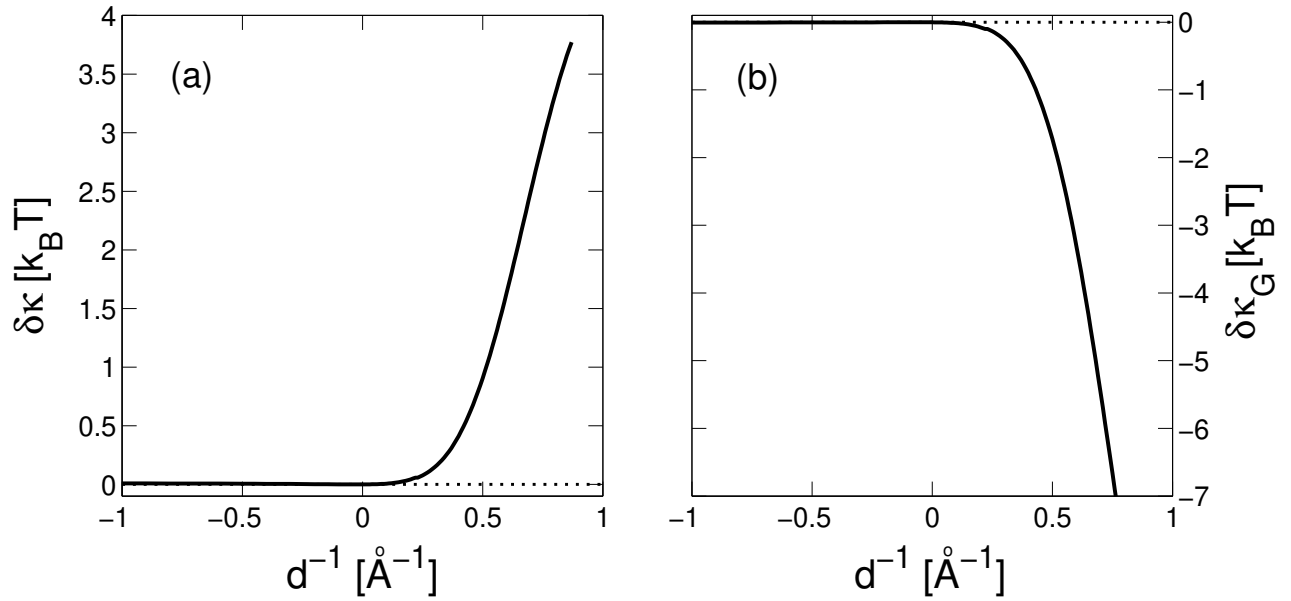


Figure 4: The  $d^{-1}$  dependence of (a)  $\delta\kappa$  and (b)  $\delta\kappa_G$  is presented again for low added salt concentration ( $c_{\text{salt}} = 0.1 \text{ mM}$ ) and for a wider  $d^{-1}$  range. For large  $d^{-1}$ , we see a significant increase in the magnitude of both  $\delta\kappa$  and  $\delta\kappa_G$ , amounting to several  $k_B T$ , which is very significant in comparison to normal membrane curvature moduli.

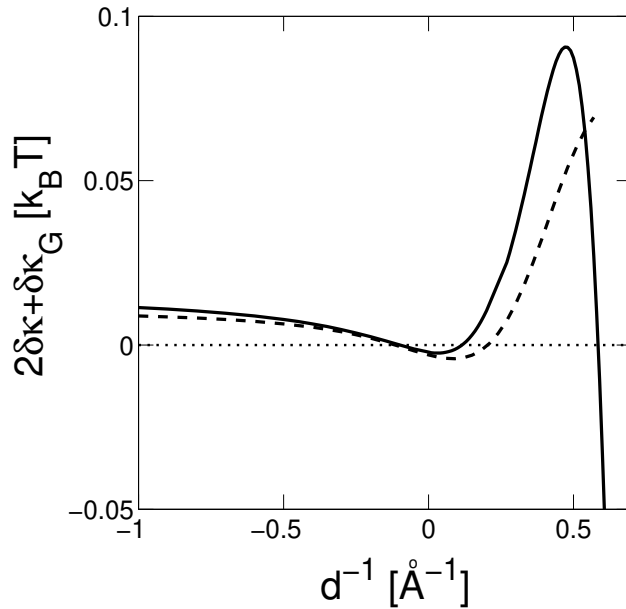


Figure 5: The contribution to the vesiculation stability  $2\delta\kappa + \delta\kappa_G$  is plotted against the short-range interaction strength  $d^{-1}$  for two amounts of added salt. The solid line is for  $c_{\text{salt}} = 0.1 \text{ mM}$  while the dashed line is for  $c_{\text{salt}} = 0.1 \text{ M}$ . As can be seen, the dashed line is positive and low for  $d^{-1} < 0$ , then becomes negative for low  $d^{-1}$ , and then positive again. The solid line has a smaller region of negative  $2\delta\kappa + \delta\kappa_G$  at low  $d^{-1}$ , but has another such region for very large  $d^{-1}$ . In this region,  $2\delta\kappa + \delta\kappa_G$  decreases strongly, and reaches negative values of order  $\sim 1k_B T$

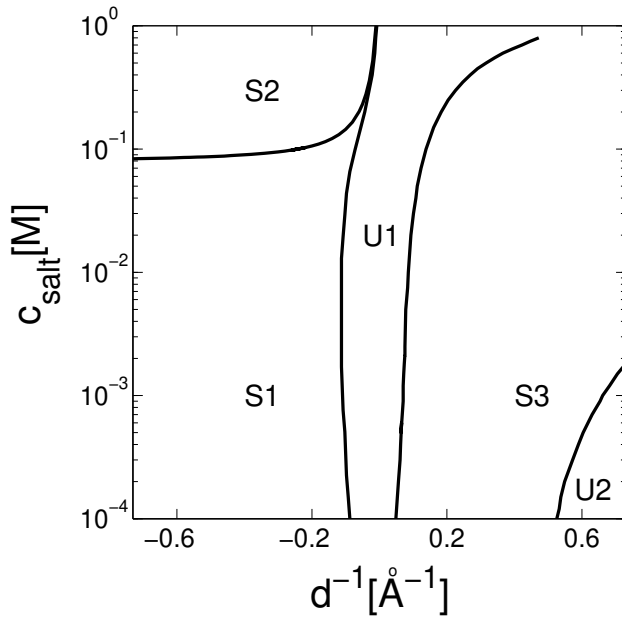


Figure 6: The phase diagram of the contribution to the vesiculation stability  $2\delta\kappa + \delta\kappa_G$  is presented, showing all five regimes. For low amounts of added salt and strongly repulsive membranes, the electrostatic adsorption of PEs increases  $2\delta\kappa + \delta\kappa_G$  (regime S1). For higher amounts of added salt, the PEs deplete, but the adsorption of salt ions still increases  $2\delta\kappa + \delta\kappa_G$  (S2). For low  $d^{-1}$ , both  $2\delta\kappa + \delta\kappa_G$  and  $\delta\kappa$  become negative (U1), for intermediate positive  $d^{-1}$   $2\delta\kappa + \delta\kappa_G$  becomes positive again (S3), and for very high  $d^{-1}$  and low salt it decreases (U2), even though  $\delta\kappa > 0$ . In all calculations we used  $|\sigma| = 10^{-4} \text{\AA}^{-2}$ . Other parameters are the same as in Fig. 1.